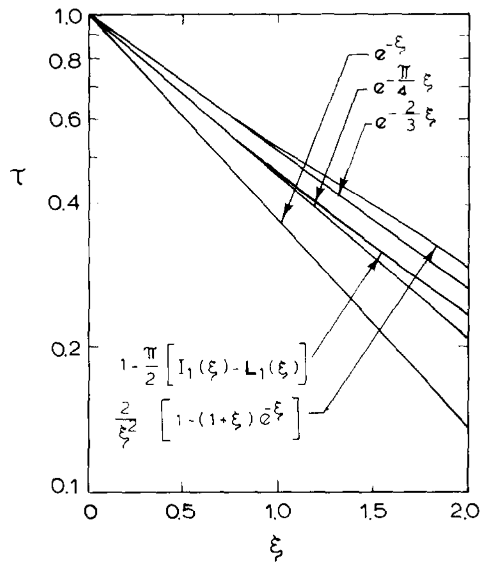


FIG. 2. $\tau$ vs $\xi$ and asymptotes.

The integral on the RHS of equation (8) is the Laplace transform of the following function

$$f(L) = \begin{cases} L(D^2-L^2)^{-1/2}; & 0 < L < D, \\ 0; & L < D, \end{cases} \tag{9}$$

and can be evaluated as [3]

$$\int_0^D \frac{e^{-kL} L \, dL}{\sqrt{(D^2-L^2)}} = D - \frac{\pi D}{2}[I_1(\xi) - \mathscr{L}_1(\xi)], \tag{10}$$

where $\xi = kD$, $I_1(\xi)$ is the modified Bessel function of order 1, and $\mathscr{L}_1(\xi)$ is the modified Struve function of order 1. Thus, we obtain

$$\tau_{\text{cylinder}} = 1 - \frac{\pi}{2}[I_1(\xi) - \mathscr{L}_1(\xi)]. \tag{11}$$

For various values of $\xi$, $\tau_{\text{cylinder}}$ was calculated by using a table of $I_1(\xi)$ and $\mathscr{L}_1(\xi)$ from ref. [4], and is plotted in Fig. 2.

The transmittance for a plane of thickness $D$ (or a cube of side $D$) when the radiation is incident normal to a face, and a sphere of diameter $D$ are given for comparison in Fig. 2. It should be noted that the transmittance of radiation for a sphere for collimated and diffuse radiation is identical so that $\tau$ for the sphere is given by the well-known [1, 2] relation

$$\tau_{\text{sphere}} = \frac{2}{\xi^2}[1-(1+\xi)e^{-\xi}]. \tag{12}$$

The negative slopes of $\tau$ at the origin (see Fig. 2) are equal to $L_0/D$, or in agreement with the predictions of equation (3), $\pi/4$ for a cylinder, 1 for a slab (or cube), and 2/3 for a sphere.

It can be seen that the error in $\tau$ of approximating it by $e^{-kL_0}$ over the range of interest in many practical situations ($kD < 2$) is zero for a slab, and less than 11% for a cylinder and a sphere. The recommendation is therefore made that in the absence of an exact formulation the transmittance of any objective may be adequately approximated for $kD < 2$ by

$$\tau = e^{-kV/A_p}. \tag{13}$$

A lower average error over the interval $0 < kD < 2$ can be obtained by using a smaller mean beam length for the cylinder and sphere, unlike the mean beam length for emission, however, no one correction factor can be defined that applies for all optical thicknesses.

*Acknowledgement*—This factor was developed for the interpretation of soot concentrations being measured as part of the United States Environmental Protection Agency Grant No. R808774.

## REFERENCES


1. H. C. Hottel and A. F. Sarofim, *Radiative Transfer*, Chapter 7. McGraw-Hill, New York (1967).
2. R. Siegel and J. R. Howell, *Thermal Radiation Heat Transfer* (2nd edn.), Chapter 17, Hemisphere, New York (1981).
3. A. Erdélyi (editor), *Tables of Integral Transform*, Vol. 1, p. 136. McGraw-Hill, New York (1954).
4. M. Abramowitz and I. A. Stegun (editors), *Handbook of Mathematical Functions with Formulas, Graphs, and Mathematical Tables*, pp. 501–502. National Bureau of Standards, Washington, DC (1964).


*Int. J. Heat Mass Transfer.* Vol. 27, No. 2, pp. 312–315, 1984
Printed in Great Britain

0017-9310/84 $3.00 + 0.00
Pergamon Press Ltd.

# UNSTEADY THREE-DIMENSIONAL MIXED CONVECTION FLOW WITH TEMPERATURE DEPENDENT VISCOSITY

C. D. SURMA DEVI† and G. NATH‡

Department of Applied Mathematics, Indian Institute of Science, Bangalore 560012, India

(*Received* 2 *August* 1982 *and in revised form* 20 *May* 1983)

## NOMENCLATURE

| | |
|---|---|
| $c$ | ratio of the velocity gradients at the edge of the boundary layer ($b/a$) when $t^* = 0$ |
| $C_f, \bar{C}_f$ | skin-friction coefficients at the wall in the $x$- and $y$-directions, respectively |
| $F, S$ | dimensionless velocity components in the $x$- and $y$-directions, respectively |
| $F'_w, S'_w$ | skin-friction parameters in the $x$- and $y$-directions, respectively |
| $G, G'_w$ | dimensionless temperature and heat transfer parameter at the wall, respectively |
| $Gr, N$ | Grashof number and ratio of viscosity, respectively |
| $Nu, Pr$ | Nusselt and Prandtl numbers, respectively |
| $t^*$ | dimensionless time |

†Present address: Department of Mathematics, Central College, Bangalore University, Bangalore 560001, India.
‡To whom correspondence should be addressed.

$T, T_{w0}, T_\infty$ temperature, wall temperature at $t^* = 0$ and free stream temperature, respectively.

Greek symbols
- $\alpha$ ratio of Grashof number to Reynolds number squared
- $\eta, \lambda$ dimensionless independent variable and parameter, respectively
- $\mu$ viscosity.

Superscript
- ′ differentiation with respect to $\eta$.

Subscripts
- e, w conditions at the edge of the boundary layer and on the surface, respectively
- $t^*$ derivatives with respect to $t^*$.

## INTRODUCTION

In recent years, mixed convection flows with constant fluid properties over two-dimensional (2-D), axisymmetric and three-dimensional (3-D) bodies have been studied and the relevant references are given in ref. [1]. But the unsteady mixed convection flow of water with temperature dependent viscosity and Prandtl number on 3-D bodies has not been studied so far.

The aim of this analysis is to study the effect of temperature-dependent viscosity and Prandtl number on the unsteady laminar incompressible mixed convection flow of water at the stagnation point of a 3-D body where the unsteadiness in the flow field is introduced by the time-dependent free stream velocity, wall temperature, and surface mass transfer. Both semi-similar and self-similar flows have been considered. The appropriate governing equations have been solved numerically using an implicit finite-difference scheme [2].

## GOVERNING EQUATIONS

The appropriate changes are incorporated in the equations of ref. [1] to take into account the variation of viscosity and Prandtl number with temperature as given in ref. [3]. The relevant equations in dimensionless form can be expressed as [1]

$$(NF')' + \varphi[(f+cs)F' + 1 - F^2] + \varphi^{-1}\varphi_{t^*}(1-F) - F_{t^*} + \varphi^{-1}\alpha G = 0, \quad (1a)$$

$$(NS')' + \varphi[(f+cs)S' + c(1-S^2)] + \varphi^{-1}\varphi_{t^*}(1-S) - S_{t^*} + \varphi^{-1}\alpha G = 0, \quad (1b)$$

$$(Pr^{-1}NG')' + \varphi(f+cs)G' - G_{t^*} = 0. \quad (1c)$$

The boundary conditions are given by

$$F = S = 0, \quad G = \varphi_1(t^*) \text{ at } \eta = 0, \qquad F = S = 1, \quad G = 0 \text{ as } \eta \to \infty, \qquad \text{for } t^* \geqslant 0. \quad (2)$$

It is assumed here that the flow is initially ($t^* = 0$) steady and changes to unsteady for $t^* > 0$. Therefore, the initial conditions are given by the steady-flow equations obtained by putting

$$\varphi(t^*) = \varphi_1(t^*) = 1, \quad \varphi_{t^*} = F_{t^*} = S_{t^*} = G_{t^*} = 0, \quad (3)$$

in equation (1).

Here

$$\eta = (\rho a/\mu_e)^{1/2} z, \quad t^* = at, \quad u_e = ax\varphi(t^*),$$
$$v_e = by\varphi(t^*), \quad u = u_e F(\eta, t^*), \quad (4a)$$
$$v = v_e S(\eta, t^*), \quad w = -(\mu_e a/\rho)^{1/2}[\varphi(t^*)(f+cs)],$$
$$G(\eta, t^*) = (T - T_\infty)/(T_{w0} - T_\infty), \quad c = b/a, \quad \alpha = Gr/Re_L^2,$$

$$Re_L = \rho a L^2/\mu_e, \quad Gr = \rho\beta g(T_{w0} - T_\infty)L^3/\mu_e, \quad (4b)$$

$$N = \mu/\mu_e = (b_1 + b_2 T_\infty)/(b_1 + b_2 T) = (1 + \alpha_1 \Delta T_{w0} G)^{-1},$$
$$\Delta T_{w0} = T_{w0} - T_\infty, \quad \alpha_1 = b_2/(b_1 + b_2 T_\infty), \quad (4c)$$
$$b_1 = 0.3471, \quad b_2 = 0.0244,$$

$$Pr = \mu c_p/k = 455/[32 + 1.8(T_\infty + \Delta T_{w0} G)],$$
$$f = \int_0^\eta F\,d\eta + f_w, \quad s = \int_0^\eta S\,d\eta, \quad f_w = A\varphi^{-1}(t^*), \quad (4d)$$
$$A = -(w_w/\bar{u}_e)(Re_x)^{1/2}, \quad Re_x = \rho a x^2/\mu_e, \quad \bar{u}_e = ax.$$

The variation of viscosity ($\mu$) and Prandtl number ($Pr$) with temperature ($T$) in the range $4.4°C \leqslant T \leqslant 37.8°C$ is represented by equations (4c) and (4d), respectively. Here $\varphi$ and $\varphi_1$ are arbitrary functions of $t^*$ representing the nature of unsteadiness in the inviscid flow and wall temperature, respectively. Also $\alpha > 0$ for $T_{w0} > T_\infty$ (i.e. for aiding force) and $\alpha < 0$ for $T_{w0} < T_\infty$ (i.e. for opposing force).

The skin-friction coefficients in the $x$- and $y$-directions and the heat transfer coefficient can be expressed in the form [1]

$$C_f = 2(Re_x)^{-1/2}\varphi(t^*)F'_w, \quad Nu = (Re_x)^{1/2}G'_w,$$
$$\bar{C}_f = 2(Re_x)^{-1/2}(v_e/u_e)\varphi(t^*)S'_w. \quad (5)$$

*Self-similar equations*

The self-similar solution to the foregoing problem exists and the governing equations in dimensionless form can be expressed as [1]

$$(NF')' + (f+cs)F' + 1 - F^2 + \lambda(1 - F - 2^{-1}\eta F') + \alpha G = 0, \quad (6a)$$

$$(NS')' + (f+cs)S' + c(1-S^2) + \lambda(1 - S - 2^{-1}\eta S') + \alpha G = 0, \quad (6b)$$

$$(Pr^{-1}NG')' + (f+cs)G' - \lambda(2G + 2^{-1}\eta G') = 0. \quad (6c)$$

The boundary conditions are given by

$$F = S = 0, \quad G = 1 \text{ at } \eta = 0; \qquad F = S = 1, \quad G = 0 \text{ as } \eta \to \infty, \quad (7)$$

where

$$\eta = (\rho a/\mu_e)^{1/2}\varphi_2^{-1/2} z, \quad \varphi_2 = 1 - \lambda t^*, \quad \lambda < t^{*-1},$$
$$u_e = ax\varphi_2^{-1}, \quad v_e = by\varphi_2^{-1}, \quad u = u_e F, \quad (8a)$$
$$v = v_e S, \quad w = -(\mu_e a/\rho)^{1/2}(f+cs)\varphi_2^{-1/2},$$
$$(T - T_\infty)/(T_{w0} - T_\infty) = \varphi_2^{-2} G,$$
$$(T_w - T_\infty)/(T_{w0} - T_\infty) = \varphi_2^{-2}, \quad (8b)$$
$$f_w = A, \quad A = -[w_w/(\mu_e a/\rho)^{1/2}]\varphi_2^{1/2}.$$

If the normal velocity at the wall $(w)_w$ is assumed to vary as $\varphi_2^{-1/2}$ and $\mu_e a/\rho$ is considered as a constant, then $f_w = A$ is a constant. Also the flow at the edge of the boundary layer is accelerating or decelerating according to whether $\lambda \gtrless 0$.

## RESULTS AND DISCUSSION

*Semi-similar case*

For computation, the free stream velocity and wall temperature distributions have been taken to be of the form $\varphi = 1 + \varepsilon t^{*2}$ and $\varphi_1 = 1 - \varepsilon_1 t^*$, respectively. Since most 3-D bodies of practical interest lie between a cylinder ($c = 0$) and a sphere ($c = 1$), this study has been confined to the range $0 \leqslant c \leqslant 1$.

Here, only the effect of variable fluid properties is stressed but in order to bring out the difference between the results with variable and constant fluid properties, the skin-friction and heat transfer results ($F'_w, S'_w, -G'_w$) for both variable and constant fluid properties are shown in Figs. 1–3. The results

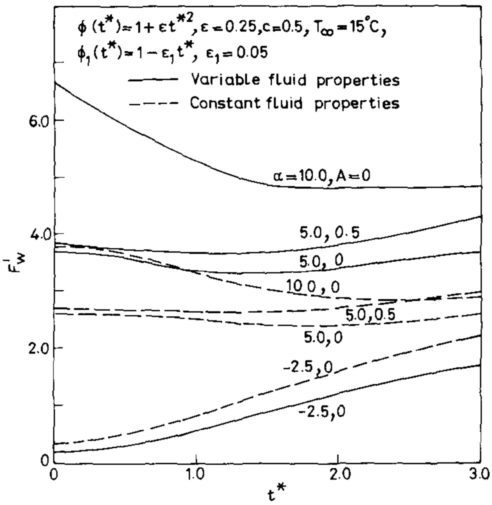


FIG. 1. Skin-friction parameter in the $x$-direction (semi-similar flow).

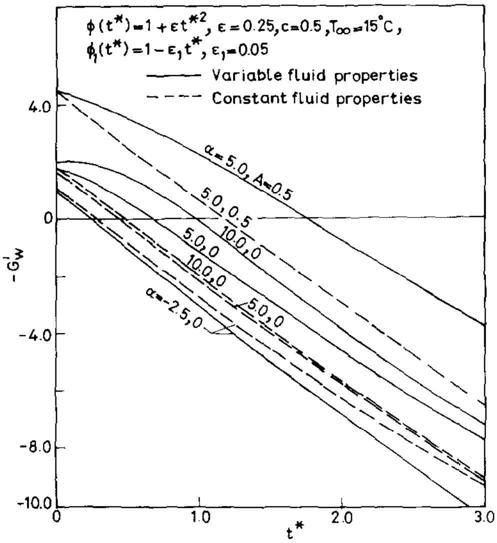


FIG. 3. Heat transfer parameter (semi-similar flow).

indicate that there is a significant difference in the two results and this difference becomes more pronounced for large values of the buoyancy parameter $\alpha$. For example, when $\alpha = 10$, the skin-friction parameters $F'_w$ and $S'_w$ for variable fluid properties differ from those of constant fluid properties by about 80% when $t^* = 0$ and by 60% when $t^* = 3$ (Figs. 1 and 2). However, the corresponding difference in heat transfer $-G'_w$ (Fig. 3) is comparatively less (about 11% at $t^* = 0$ and about 25% at $t^* = 3$). Also, the effect of the buoyancy parameter is more pronounced for variable fluid properties than for constant fluid properties. For an opposing force ($\alpha < 0$), the values of the skin-friction and heat transfer parameters ($F'_w, S'_w, -G'_w$) for constant fluid properties are more than those of variable fluid properties. On the other hand, for aiding force ($\alpha > 0$), it is the other way around. The effect of mass transfer $A$ is found to be more pronounced on the heat transfer ($-G'_w$) than on the skin friction ($F'_w, S'_w$). This is true for both variable and constant fluid property cases (Figs. 1–3). Therefore, it can be concluded that the effect of variable fluid properties has to be taken into account for water especially for large buoyancy parameters in order to predict skin friction and heat transfer accurately.

*Self-similar case*

For this case, the governing equations (6a)–(6c) under boundary conditions (7) have been solved by the same method used for the semi-similar case and the results ($F'_w, S'_w, -G'_w$) are presented in Figs. 4–6. The difference between the results corresponding to variable and constant fluid properties is qualitatively and to some extent quantitatively similar to those of the semi-similar flow results. For example, when $\alpha = 10$, the difference between the skin-friction results ($F'_w, S'_w$) for variable and constant fluid properties is about 60% for $\lambda = -1$ (decelerating flow) and 90% for $\lambda = 1$ (accelerating flow), but the difference between the heat transfer results is about 50% for $\lambda = -1$ and about 3% for $\lambda = 1$.

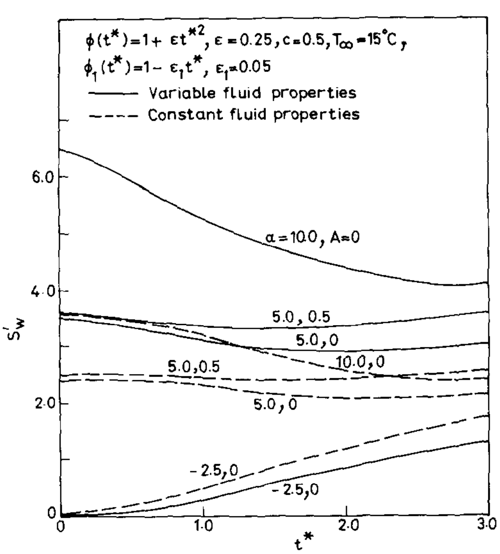


FIG. 2. Skin-friction parameter in the $y$-direction (semi-similar flow).

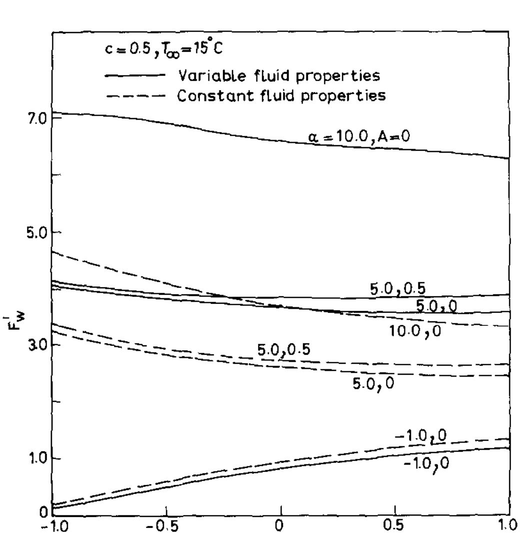


FIG. 4. Skin-friction parameter in the $x$-direction (self-similar flow).

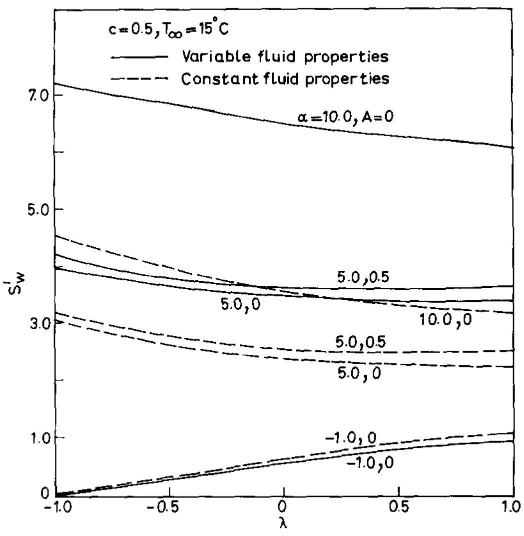


FIG. 5. Skin-friction parameter in the $y$-direction (self-similar flow).

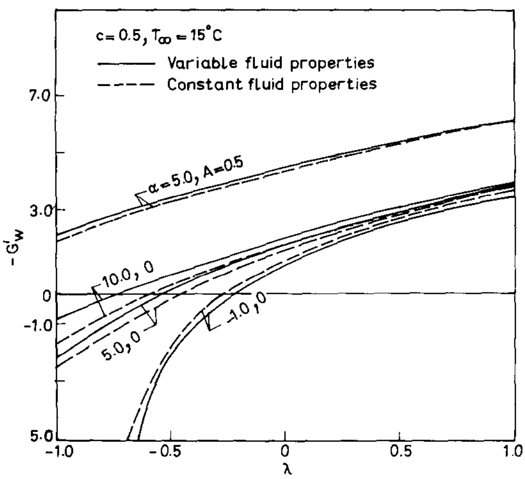


FIG. 6. Heat transfer parameter (self-similar flow).

## CONCLUSIONS

The skin friction and heat transfer are found to be strongly dependent on the variation of viscosity and Prandtl number with temperature especially for large values of buoyancy forces. The effect of mass transfer is found to be more pronounced on the heat transfer than on the skin friction.

## REFERENCES

1. M. Kumari and G. Nath, Unsteady mixed convection near the stagnation point in three-dimensional flow, *J. Heat Transfer* **104**, 132–138 (1982).
2. J. G. Marvin and Y. S. Sheaffer, A method for solving nonsimilar laminar boundary-layer equations including foreign gas injection, *NASA Tech. Note* D-5516 (1969).
3. L. S. Yao, Variable viscosity effect on the laminar water boundary layer on heated cones, *J. Appl. Mech.* **45**, 481–486 (1978).

*Int. J. Heat Mass Transfer.* Vol. 27, No. 2, pp. 315–317, 1984
Printed in Great Britain

0017 9310/84 $3.00 + 0.00
Pergamon Press Ltd.

# THE EXISTENCE OF NUCLEATE BOILING IN DIABATIC TWO-PHASE ANNULAR FLOW

D. R. H. BEATTIE and W. J. GREEN

Nuclear Technology Division, AAEC, Lucas Heights Research Laboratories,
New Illawarra Road, Lucas Heights, NSW, Australia

(*Received* 24 *April* 1983)

DURING recent years, there has been much speculation on the possible existence of nucleate boiling in high quality diabatic annular flows [1–7]. Hypotheses have been formulated and experimental data re-analysed [1, 2] in an effort to show that nucleate boiling may occur in the liquid film region at the wall. A recent paper [7] describes experiments designed especially to test the hypothesis of annular flow nucleate boiling, and involving the determination of heat transfer coefficients at constant quality and film flow. Data were obtained using a tube, 367.2 cm long by 9.6 mm diameter, the first 182.9 cm of which was heated to produce a desired quality for a given flow; the next 138.6 cm (or 144 diameters) was unheated to ensure flow development; and the last heated 45.7 cm was the section in which heat transfer coefficients were determined. The heat transfer characteristics were determined from wall temperatures monitored by seven thermocouples uniformly spaced along the final section, power input measurements, and local coolant conditions. Experiments were performed with steam–water at near atmospheric pressure; mass fluxes were 105 and 203 $kg\,m^{-2}\,s^{-1}$, and qualities ranged from 0.05 to 0.42.

On the basis of linear relationships between heat flux and wall superheat at constant mass flows and qualities, Aounallah *et al.* [7] concluded that nucleate boiling was not present for the range of annular flow conditions covered by their experiments.

This communication draws attention to similar experiments performed nearly two decades ago, by Bertoletti *et al.* [8] whose results were at variance with the conclusions of Aounallah *et al.*

Bertoletti *et al.* [8] heated water at a pressure of 7 MPa to required coolant qualities in an electrically heated section corresponding to the 182.9 cm preheated section used in the more recent experiments [7]. Heat transfer measurements were made near the inlets and exits of two heated tubes 80 cm long by 4.99 mm diameter and 139.9 cm long by 9.18 mm diameter, respectively. In each case the heated test section was